

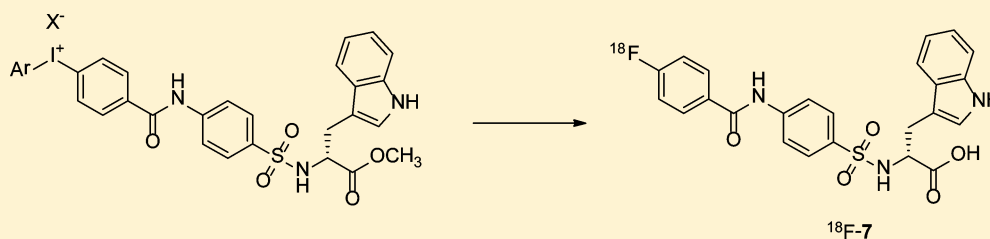
Design, Synthesis, and Initial Evaluation of a High Affinity Positron Emission Tomography Probe for Imaging Matrix Metalloproteinases 2 and 9

Svetlana V. Selivanova,^{*,†,||} Timo Stellfeld,^{‡,||} Tobias K. Heinrich,[‡] Adrienne Müller,[†] Stefanie D. Krämer,[†] P. August Schubiger,[†] Roger Schibli,[†] Simon M. Ametamey,^{*,†} Bernhard Vos,[‡] Jörg Meding,[‡] Marcus Bauser,[‡] Joachim Hütter,[‡] and Ludger M. Dinkelborg^{‡,§}

[†]Center for Radiopharmaceutical Sciences, ETH Zurich, CH-8093 Zurich, Switzerland

[‡]Global Drug Discovery, Bayer Healthcare, 13353 Berlin, Germany

S Supporting Information



ABSTRACT: The activity of matrix metalloproteinases (MMPs) is elevated locally under many pathological conditions. Gelatinases MMP2 and MMP9 are of particular interest because of their implication in angiogenesis, cancer cell proliferation and metastasis, and atherosclerotic plaque rupture. The aim of this study was to identify and develop a selective gelatinase inhibitor for imaging active MMP2/MMP9 *in vivo*. We synthesized a series of *N*-sulfonylamino acid derivatives with low to high nanomolar inhibitory potencies. (*R*)-2-(4-(4-Fluorobenzamido)phenylsulfonamido)-3-(1*H*-indol-3-yl)propanoic acid (**7**) exhibited the best *in vitro* binding properties: MMP2 $IC_{50} = 1.8$ nM, MMP9 $IC_{50} = 7.2$ nM. Radiolabeling of **7** with no carrier added ^{18}F -radioisotope was accomplished starting from iodonium salts as precursors. The radiochemical yield strongly depended on the iodonium counteranion ($ClO_4^- > Br^- > TFA^- > tosylate$). ^{18}F -**7** was obtained in up to 20% radiochemical yield (decay corrected), high radiochemical purity, and >90 GBq/ μ mol specific radioactivity. The radiolabeled compound showed excellent stability *in vitro* and in mice *in vivo*.

■ INTRODUCTION

Matrix metalloproteinases (MMPs) are extracellular enzymes which are synthesized in the rough endoplasmic reticulum and excreted into the extracellular space as inactive pro-forms.¹ Activation of the excreted MMPs by proteolytic cleavage results in the exposure of the catalytic domain containing a Zn^{2+} ion. Tissue inhibitors of metalloproteinases (TIMPs) serve as endogenous MMP inhibitors and control the amount of active enzyme by blocking its catalytic site. The activity of several MMPs is elevated locally during many pathologies, for example, cancer, atherosclerosis, and chronic inflammatory diseases, as a result of a disrupted balance between synthesis, activation, inhibition, and degradation. Noninvasive imaging of increased MMP activity could aid early diagnosis of a pathological state.

Targeting activated MMPs can be achieved with appropriate MMP substrates or inhibitors. The substrates, which are cleaved by MMP to products with altered fluorescent properties, have been evaluated for optical imaging with some success.^{2,3} However, optical imaging cannot be translated to clinical applications due to the limited depth of tissue penetration by light. MMP inhibitors interact with the enzyme at the catalytic site in a stoichiometric fashion and allow

quantification of active MMPs by high-sensitivity imaging. Positron emission tomography (PET) offers noninvasive quantitative analysis at nanomolar concentrations both, in preclinical and clinical settings.

Several research groups attempted to develop PET probes for active MMPs based on inhibitors.^{4–10} A decade ago, a range of ^{18}F - or ^{11}C -radiolabeled sulfonamides **1–3** (Figure 1) were reported.^{5–7} Despite promising *in vitro* results, none of the proposed tracers was advanced further as an imaging agent. Selected analogue **4** (Figure 1) was evaluated in breast cancer mouse models but did not significantly accumulate in the MCF-7 transfected with IL-1 α or MDA-MB-435 xenografts.⁸ Very recently, novel MMP inhibitors were introduced having the pyrimidine-2,4,6-trione (**5**, Figure 1) structural core.^{9,10} Preliminary PET experiments using **5** in healthy mice showed low background radioactivity in nontargeted tissues, but clearance was slower than desired for an ^{18}F -labeled tracer.⁹ It should be noted that all of the above-mentioned compounds are broad spectrum MMP inhibitors, binding to MMP2,

Received: January 30, 2013

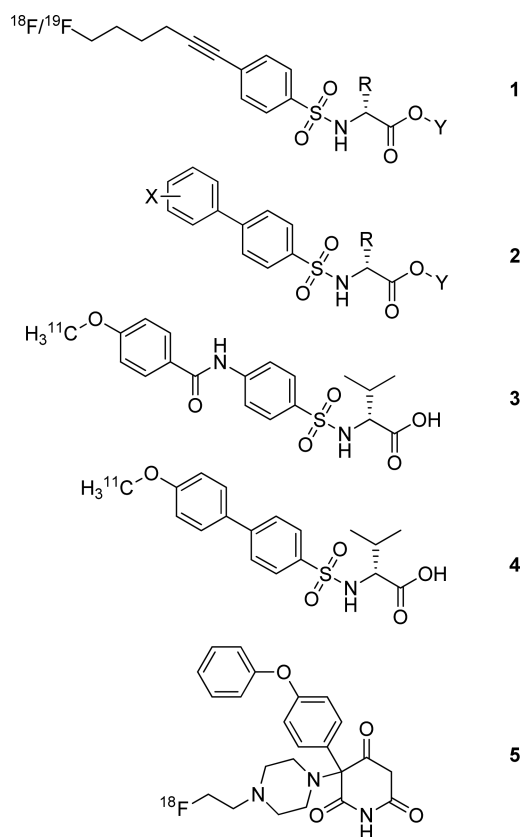


Figure 1. Previously reported radiolabeled broad spectrum MMP inhibitors. X = $^{18}\text{F}/^{19}\text{F}$, NO_2 , $\text{O}^{11}\text{CH}_3/\text{O}^{12}\text{CH}_3$; Y = OH, $\text{O}^{11}\text{CH}_3/\text{O}^{12}\text{CH}_3$; R = $\text{CH}_2\text{CH}_2\text{SCH}_3$, $\text{CH}_2(3\text{-indolyl})$, $\text{CH}_2(\text{CH}_3)_2$.

MMP8, MMP9, and MMP13. There is currently no successful MMP selective radiotracers available for the PET imaging.

Deregulation of the gelatinases MMP2 (gelatinase A, 72 kDa type IV collagenase) and MMP9 (gelatinase B, 92 kDa type IV collagenase) are of particular interest because they are implicated in angiogenesis, cancer cell proliferation and metastasis, and atherosclerotic plaque rupture. In this work, we were looking to identify and develop a selective MMP2/MMP9 inhibitor for imaging and quantification of gelatinase activity *in vivo* by PET. We synthesized a series of novel compounds containing (R)-3-(1H-indol-3-yl)-2-sulfonamidopropanoic acid pharmacophore and tested their inhibitory potencies (IC_{50}) *in vitro* using a fluorescence-based assay (Table 1). MMP2/MMP9 inhibitor 7 was chosen as a potential PET imaging agent due to its promising binding characteristics.

Two asymmetric iodonium salt precursors were synthesized for further labeling with ^{18}F radioisotope and four different iodonium counteranions were evaluated. The radiofluorinated product, ^{18}F -7, was prepared in good and reproducible yields. Metabolites studies were performed to determine the *in vivo* stability of the radiotracer. Its clearance profile was evaluated in mice using PET.

RESULTS AND DISCUSSION

Chemistry. A series of 14 compounds 6–19, containing (R)-3-(1H-indol-3-yl)-2-sulfonamidopropanoic acid pharmacophore, were synthesized. The preparation of the key intermediates, aniline I and aniline II, is shown in Scheme 1. The anilines were synthesized according to the published procedure.^{7,11} Compound 6 was prepared as described earlier,¹¹

and the same approach was adapted for the syntheses of analogues 7–16 (Scheme 2). Final acylation of the amine function was performed according to two different methods, using corresponding acid or acyl chloride. Compounds 17–19 were synthesized by coupling D-tryptophan methyl ester and appropriate sulfonyl chloride under basic conditions (Scheme 2). Hydrolysis of the methyl ester bond with sodium or lithium hydroxide resulted in the free acid function. The *t*-butyl ester group in compounds 13, 15, and 16 was cleaved under acidic conditions.

Synthesized compounds 6–19 were assayed for their inhibitory potencies. MMP enzyme activity was determined by recording the initial slopes of fluorescence increase, which resulted from enzymatic cleavage of an internally quenched fluorogenic substrate. MMP2 and MMP9 inhibitors were identified by a decrease in initial slopes and compared to the control reaction without the test compound. The obtained IC_{50} values are presented in Table 1. Compound 6, which was reported previously,¹¹ shows equally high binding affinity to both MMP2 and MMP9. In an attempt to shift selectivity toward MMP9, we modified the aromatic ring, adjacent to the sulfonyl moiety, by introducing different halogens and alkoxy substituents. None of the modifications we attempted resulted in MMP9 selectivity. Often, MMP2 inhibitory potency remained in a low nanomolar range, while MMP9 inhibition decreased, indicating that MMP2 is tolerant to variations in this part of the molecule. In contrast, the inhibitory potency of MMP9 was retained only when modifications on the aromatic ring were carried out with bromo, fluoro, and iodo substituents. Increasing the bulkiness and lipophilicity by replacing the methoxy substituent with *iso*-propoxy and *iso*-butoxy moieties (9–12) clearly diminished the inhibitory activity, although it remained below $1\ \mu\text{M}$. Replacement of benzene by pyridine ring (13–16) gave derivatives with slightly increased IC_{50} values for both MMPs but still in the low nanomolar range (e.g., 14). However, an exception in this series was compound 15; positioning of the fluoro-substituent in the pyridine ring *ortho* to the carbonyl group resulted in a drastic loss of affinity, which, we speculate, could be due to steric and/or electronic hindrance.^{12,13} Removal of the amide linker between the two benzene rings (17–19) was tolerated better by MMP2 than by MMP9. Selected compounds, namely, 6, 7, and 14, were tested also against MMP1. The IC_{50} values for all the three compounds for MMP1 were $>1000\ \text{nM}$. Because of a favorable inhibitory potency and the possibility of labeling the structure with ^{18}F radioisotope, we selected MMP2/MMP9 inhibitor 7 as a potential radiotracer.

Synthesis of Precursors for Radiolabeling. The introduction of nucleophilic ^{18}F -fluoride into an aromatic ring during the last steps of radiosynthesis, as required for short-lived PET tracers, is not always easy. Usually, a very good leaving group such as nitro or trimethylammonium group is needed as well as an activating electron-withdrawing group *ortho* or *para* to the leaving group. In this work, we selected an approach which utilizes arylodonium salts as precursors without the need to introduce an activating group. It is documented that arylodonium salts are highly reactive due to the excellent leaving ability of the hypervalent arylodonium group.¹⁴

The synthesis of asymmetrical iodonium salt precursors 22 and 23, having two distinct leaving groups, thiophene or anisole, proceeded according to Scheme 3. The procedure involving the oxidative formation of iodonium compounds (20,

Table 1. Chemical Structures of Derivatives 6–19 and Their Inhibitory Potencies^a

Cpd	R-	IC ₅₀ (nM), MMP2	IC ₅₀ (nM), MMP9	Cpd	R-	IC ₅₀ (nM), MMP2	IC ₅₀ (nM), MMP9
6		0.9	1	13		14	78
7		1.8	7	14		7	17
8		<1	1.1	15		141	>1000
9		<1	11	16		5.2	38
10		4.8	21	17		5.8	230
11		<1	97	18		4.8	28
12		<1	460	19		3.6	100

^aIC₅₀ values are represented as average of four independent determinations with standard deviation below 5%.

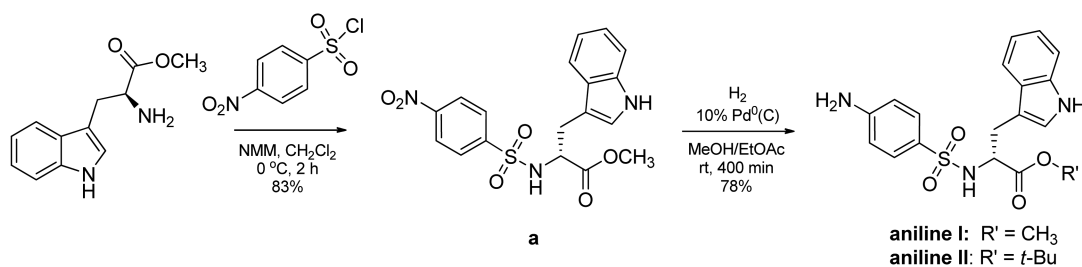
21) was adapted from the literature.¹⁵ Coupling of the resulting diaryliodonium synthon to the pharmacophore was performed under basic conditions. Purification of the iodonium salts was not trivial. Conventional workup and column chromatography resulted in partial counterion exchange due to the presence of other anions in the mobile phase. To ensure the integrity of the structure, the counterion was introduced using reversed-phase HPLC ion-exchange protocol. All iodonium salts were prepared in low to moderate yields.

Radiochemistry. Radiolabeling with nucleophilic ¹⁸F-fluoride was achieved in one step followed by deprotection of the carboxylic acid function. The reaction conditions were optimized and different leaving groups (anisole, thiophene) as well as different iodonium counteranions (bromide, perchlo-

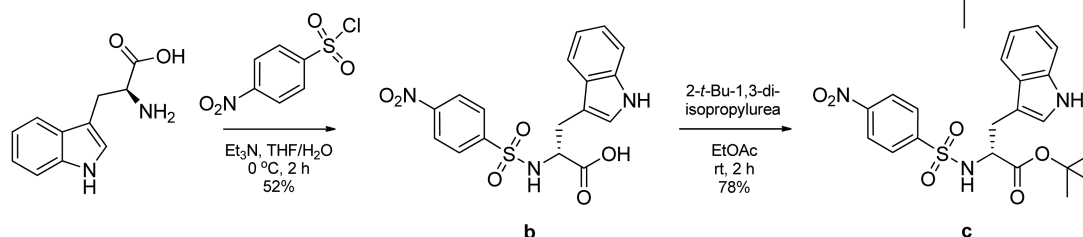
rate, trifluoroacetate, tosylate) were evaluated (Scheme 4). Thiophene and anisole leaving groups, both, were displaced by ¹⁸F in the presence of cesium carbonate in DMF containing trace amounts of water at 130 °C for 3 min. Interestingly, the radiochemical yield (RCY) was higher with a shorter reaction time: 70% fluoride incorporation was observed at 3 min, decreasing to 55% at 5 min, and further to 40% at 15 min reaction time. The reaction did not occur or gave low and unreliable yields when dry (anhydrous) solvents (acetonitrile, DMF, DMSO) were used (data not shown). Similar observations were reported in the literature.^{16,17} The exact mechanism of this reaction is still under discussion.¹³ We speculate that traces of water are beneficial because they

Scheme 1. Synthesis of Key Intermediates Aniline I and Aniline II

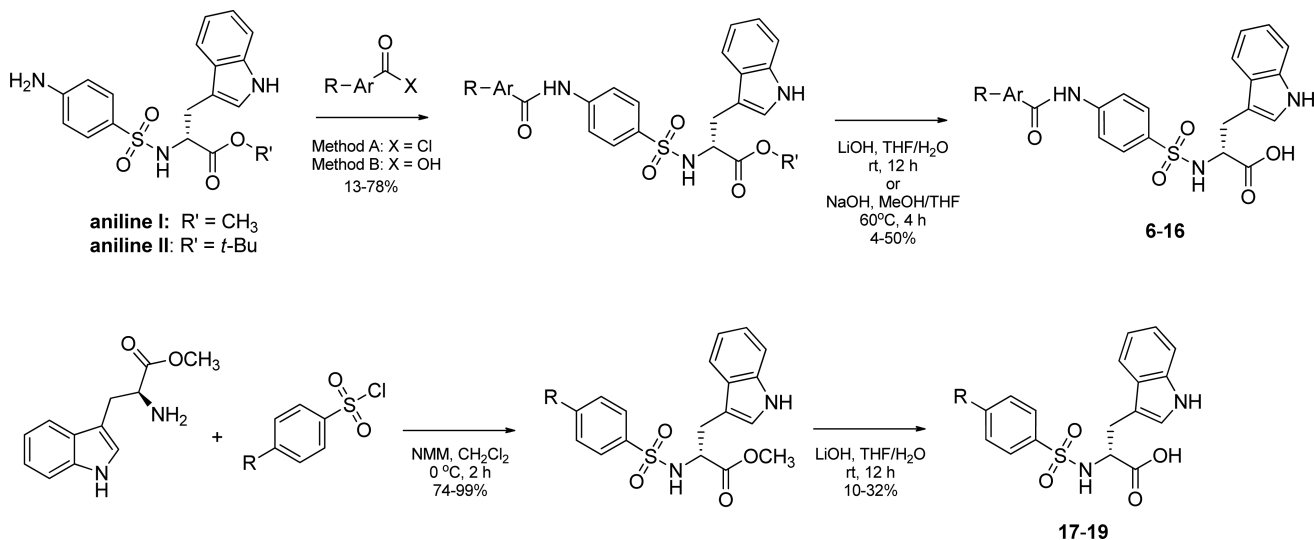
Route to aniline I:



Route to aniline II:



Scheme 2. Synthesis of Compounds 6–19

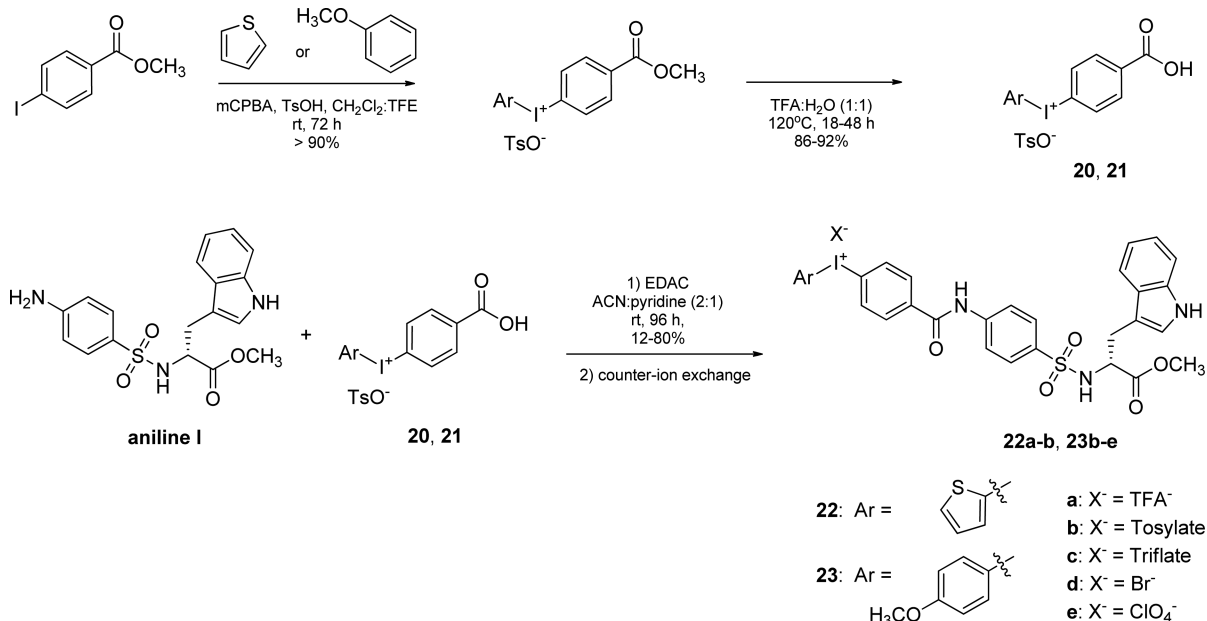
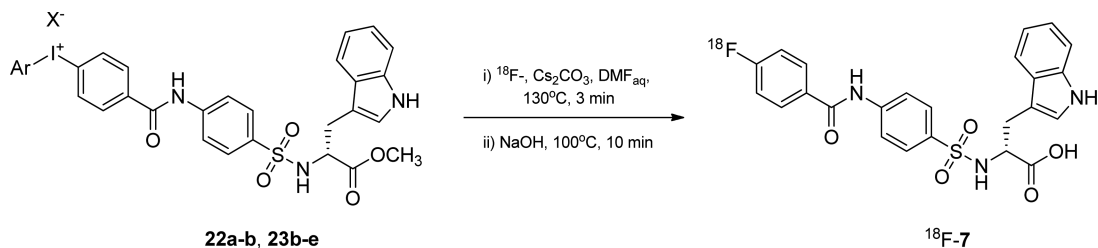


catalyze the formation of the intimate ion–molecule pair (where the molecule is *p*-iodoanisole or 2-iodothiophene), making the nonactivated aromatic ring positively charged and ready for a nucleophilic attack (Scheme 5).¹⁴ Ionizing solvent, such as water, reduces the energy required for heterolytic bond dissociation, thereby favoring this pathway over a homolytic one. The use of radical scavengers like TEMPO (2,2,6,6-tetramethylpiperidine 1-oxyl) did not improve RCY (data not shown), as was reported by others.^{18,19} This suggests that there is no important formation of radicals or they do not interfere with the radiolabeling reaction. In general, the precursor having anisole leaving group gave higher radiochemical yields than the precursors containing thiophene, thus further optimization of the reaction was performed using the anisole containing precursor. It was shown previously for small model compounds that inorganic counterions give higher RCYs.²⁰ The influence of the counteranion on RCY was evaluated under optimized

radiolabeling conditions and found to be substantial. For our heavily functionalized precursors, the RCYs were also considerably higher when inorganic counteranions were used and decreased in the following order: perchlorate > bromide > tosylate > triflate (Chart 1). We speculate that bulkier organic anions that have in addition more pronounced covalent bonding properties hinder solvolysis of an iodonium salt, limiting the formation of ion–molecule pair. Other possible reasons for the advantage of inorganic counterions are extensively discussed in the literature.²⁰

Cleavage of the methyl ester functionality was performed under basic conditions. To confirm that there was no racemization of ¹⁸F-7, we performed the same reaction on a larger scale using nonradioactive methyl ester of compound 7. Chiral HPLC confirmed the formation of the *R*-enantiomer only, which was obtained in quantitative yield, and no *S*-enantiomer could be detected, indicating that no racemization

Scheme 3. Synthesis of the Labeling Precursors

Scheme 4. Radiosynthesis of ^{18}F -7 under Optimized Reaction Conditions

Scheme 5. Formation of Intimate Ion–Molecule Pair

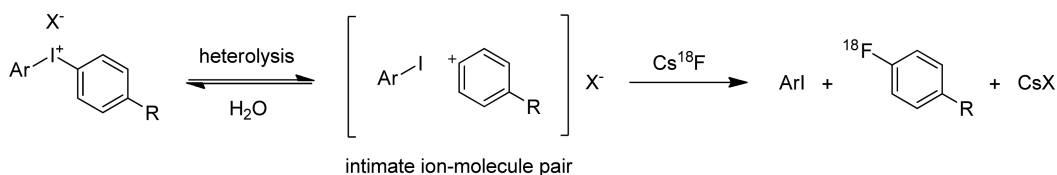
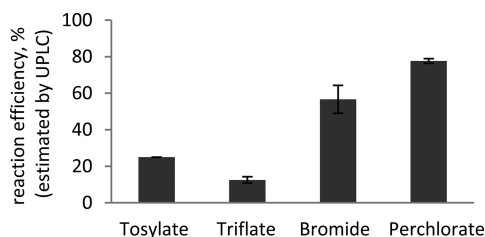


Chart 1. Influence of the Counter-Anion on the Radiolabeling Yield



of ^{18}F -7 occurred under the reaction conditions. The final product was purified using reversed-phase semipreparative HPLC. Initially, 0.1% aqueous trifluoroacetic acid (TFA) was used with acetonitrile as the mobile phase for the semipreparative HPLC. Later we found the radiolabeled product was unstable under strongly acidic conditions. For this reason, the use of TFA as an additive was discontinued and replaced by 10 mM ammonium bicarbonate buffer. ^{18}F -7 could be

reproducibly synthesized and formulated for in vivo application in 10–20% RCY (decay corrected to EOB, $n > 10$) with specific radioactivities $>90 \text{ GBq}/\mu\text{mol}$ ($>2.5 \text{ Ci}/\mu\text{mol}$) (EOS) under optimized radiolabeling and purification conditions. Radiochemical and chemical purity was $>95\%$, as confirmed by HPLC.

Metabolic Stability. The tracer ^{18}F -7 was stable in rodent and human plasma in vitro. No decomposition occurred up to 2 h of incubation at 37°C . Metabolic stability in vivo was evaluated in C57BL/6 mice. Only parent compound was identified in blood, and 85% of the radioactivity in urine corresponded to intact radiotracer 60 min after injection.

PET/CT Imaging. In a preliminary study, PET/CT scan of a C57BL/6 mouse (Figure 2) showed mainly hepatobiliary clearance of the tracer. Radioactivity was also relatively high in urinary bladder. The absence of bone uptake confirmed that there is no defluorination of the tracer in vivo.

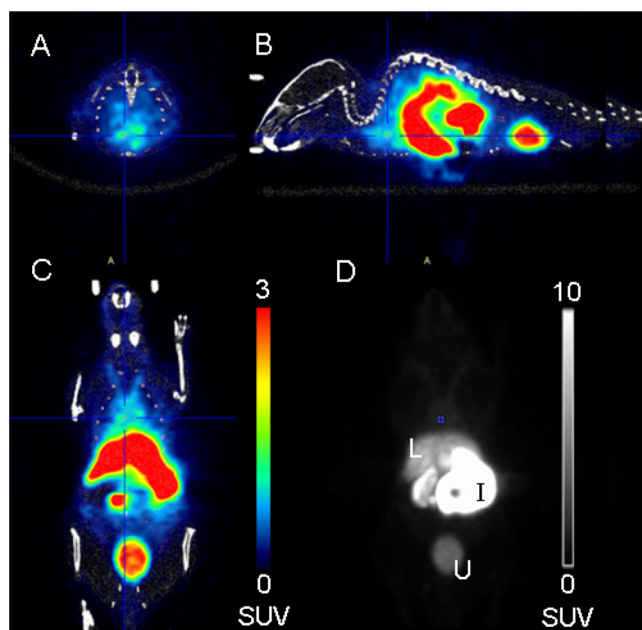


Figure 2. PET/CT image of a C57BL/6 mouse. Transversal (A), sagittal (B), and coronal (C) sections (indicated by crosshairs), averaged 8–38 min after injection of 5.3 MBq ^{18}F -7, 2 bed positions, 15 min each starting with anterior part. Color scale, PET; white, CT. PET maximum intensity projection (D). SUV, standardized uptake value; L, liver; I, intestine; U, urinary bladder.

CONCLUSION

Novel potent MMP2/MMP9 inhibitor 7 was identified based on SAR studies. The compound was radiolabeled with ^{18}F in satisfactory radiochemical yields and high specific radioactivity. ^{18}F -7 showed excellent *in vivo* stability in wild-type mice. Further evaluation of the tracer suitability for cancer and atherosclerosis imaging is in progress.

EXPERIMENTAL SECTION

All commercially available reagents and solvents were used as received. Organic reactions were monitored by TLC on normal phase silica gel plates (DC Kieselgel 60 F_{254} ; Merck). Mobile phase was a mixture of hexane and ethyl acetate at suitable ratios. Developed TLCs were visualized under UV light at 254 nm. Crude products were purified by normal phase flash column chromatography on Biotage Isolera Prime system using SNAP KP-Sil cartridges and an appropriate gradient of ethyl acetate in hexane as mobile phase. An optimal gradient was calculated automatically by Biotage Isolera Prime TLC-to-Gradient software. Reversed-phase preparative HPLC was performed on an Agilent Technologies 1200 series HPLC system using an XBridge Prep C18 OBD, particle size 5 μm , 30 mm \times 100 mm column. The mobile phase consisted of 0.1% TFA in water and acetonitrile. The acetonitrile gradient from 5% to 95% over 20 min at 30 mL/min flow rate was applied. Ion exchange was performed on Biotage Isolera using RP-18 PuriFlash 15PT C18T cartridges (Interchim) and the mobile phase as described below (see: Introduction of Counterions). The chiral HPLC system consisted of a Dionex Pump 680, ASI 100, and Waters UV-detector 2487. The enantiomers were resolved on a Chiralpak AD-H 5 μm 150 mm \times 4.6 mm column using hexane/ethanol 70/30 + 0.1% diethylamine as solvent at a flow rate of 1.0 mL/min and UV detection at 254 nm. NMR spectra were recorded on Bruker Avance 300 (frequencies: ^1H , 300 MHz; ^{13}C , 75 MHz) or Bruker Avance 400 (frequencies: ^1H , 400 MHz; ^{13}C , 100 MHz) spectrometers with the corresponding residual solvent signals as an internal standard (CDCl_3 : ^1H NMR at δ 7.26, ^{13}C NMR at δ 77.23. D_2O : ^1H NMR at δ 4.8. $\text{DMSO}-d_6$: ^1H NMR at δ 2.5, ^{13}C NMR at δ 39.51). For ^{19}F -NMR,

FCCL_3 was used as an internal standard (δ 0.0). Low-resolution mass spectra (MS) were recorded on a Waters ZQ 4000 mass spectrometer. High-resolution mass spectra (HRMS) were recorded on a Waters Q-TOF Premier mass spectrometer. Optical rotations were recorded on a Jasco P-2000 polarimeter. Radiolabeling reactions were monitored and radiometabolites were detected using UPLC. The system was Acquity UPLC from Waters, equipped with a FlowStar LB 513 radiodetector (Berthold Technologies) and a UPLC dedicated reversed-phase Acquity BEH C18, particle size 1.7 μm , 100 mm \times 2.1 mm column. The mobile phase consisted of a gradient of acetonitrile in water with 0.1% TFA or a gradient of acetonitrile in aqueous 10 mM NH_4HCO_3 buffer (pH 8) from 5% to 95% over 2 min, flow rate 0.7 mL/min. Semipreparative HPLC for radiolabeled product purification was carried out on an HPLC system equipped with a Merck–Hitachi L-6200A intelligent pump, a 5 mL injection loop, a Knauer Variable Wavelength Monitor UV detector, and an Eberline RM-14 radiodetector on a reversed-phase Phenomenex Gemini C18 column, particle size 5 μm , 250 mm \times 10 mm. The mobile phase consisted of isocratic 40% acetonitrile/60% 10 mM NH_4HCO_3 buffer (pH 8) v/v, eluted at 4 mL/min flow rate. UV absorbance was detected at 254 nm. Analytical HPLC was performed on an Agilent 1100 series system equipped with a Raytest Gabi Star radiodetector. Analytical reversed-phase column was Phenomenex Luna C18, particle size 5 μm , 250 mm \times 4.6 mm. A gradient of acetonitrile in aqueous 10 mM NH_4HCO_3 buffer (pH 8) from 5% to 95% over 20 min at a flow rate of 1 mL/min was used. The synthesized compounds were characterized by ^1H , ^{13}C , ^{19}F NMR, MS, and HPLC. Purity was exceeding 95%, unless specified otherwise.

Chemistry. *Acylation of Anilines I, II: General Procedure. Method A.* The aniline was dissolved in dichloromethane (10 mL) and *N*-methylmorpholine (2 equiv) was added at 0 $^\circ\text{C}$ followed by acyl chloride (1.5 equiv). The reaction was slowly warmed to room temperature. After 12 h, the reaction mixture was poured into water (20 mL) and extracted with ethyl acetate (3 \times 20 mL). The organic phases were combined, washed with brine (20 mL), dried (MgSO_4), and concentrated. The crude product was purified by flash column chromatography on silica gel with hexane/ethyl acetate as eluent.

Method B. The carboxylic acid (2 equiv) was dissolved in DMF (2 mL/mmol carboxylic acid) and *O*-(7-azabenzotriazol-1-yl)-*N,N,N',N'*-tetramethyluronium hexafluorophosphate (HATU, 2 equiv, 0.5 M solution in DMF), 1-hydroxy-7-azabenzotriazole (HOAt, 2 equiv, 0.5 M solution in DMF) and *N,N*-diisopropylethylamine (DIPEA, 4 equiv, 1 M solution in DMF) were added consequently. After 5 min, the aniline (1 equiv) was added and the mixture was stirred for 3 h. The reaction was poured into water (20 mL) and extracted with ethyl acetate (3 \times 20 mL), and the combined organic phases were washed with 1N aqueous HCl (20 mL), 1N NaHCO_3 (2 \times 20 mL), dried (MgSO_4), and concentrated. The crude product was purified by reversed-phase column chromatography with acetonitrile/water as eluent.

Deprotection of Carboxylic Acid Function: General Procedure. The α -sulfonylamino methyl ester was dissolved in THF/water (1:1, 5 mL) and LiOH was added. The solution was stirred at room temperature for 12 h. The mixture was poured into 1N aqueous HCl (30 mL) and extracted with ethyl acetate (3 \times 20 mL). The organic phases were combined, washed with brine (20 mL), dried (MgSO_4), and concentrated. The crude product was purified by preparative reversed-phase HPLC using water/acetonitrile as eluent.

(R)-2-[4-(4-Fluoro-benzoylamino)-benzenesulfonylamino]-3-(1H-indol-3-yl)-propionic Acid (7). Aniline I (198 mg, 0.53 mmol) was reacted with 4-fluorobenzoyl chloride (95 μL , 0.80 mmol) according to method A to yield the corresponding amide (182 mg, 0.37 mmol, 69%). A part of the resulted methyl ester (50 mg, 0.1 mmol) was dissolved in MeOH/THF (1:1, 3 mL), and 0.5 mL 1N aqueous NaOH was added. The solution was stirred for 4 h at 60 $^\circ\text{C}$ and cooled to room temperature. The mixture was poured into 1N aqueous HCl (20 mL) and extracted with ethyl acetate (3 \times 20 mL). The organic phases were combined, washed with brine (20 mL), dried (MgSO_4), and concentrated. Purification by preparative reversed-phase HPLC gave the title compound (19 mg, 0.04 mmol, 39%);

$[\alpha]^{20}_D -22.6^\circ \pm 1.32^\circ$ (c 0.10, DMSO). ^1H NMR (400 MHz, DMSO- d_6) δ , ppm: 10.77–10.86 (m, 1H), 10.53 (s, 1H), 8.15 (d, J = 8.59 Hz, 1H), 8.05 (dd, J = 5.56, 8.84 Hz, 2H), 7.81–7.87 (m, 2H), 7.58–7.63 (m, 2H), 7.40 (t, J = 8.84 Hz, 2H), 7.30 (t, J = 8.34 Hz, 2H), 7.08 (d, J = 2.27 Hz, 1H), 7.02 (t, J = 8.08 Hz, 1H), 6.90–6.96 (m, 1H), 3.88–3.95 (m, 1H), 3.05 (dd, J = 6.82, 14.40 Hz, 1H), 2.86 (dd, J = 7.58, 14.40 Hz, 1H). ^{13}C NMR (101 MHz, DMSO- d_6) δ , ppm: 172.5, 165.5, 164.8, 163.0, 158.0, 142.4, 136.0, 135.2, 131.0, 130.6, 130.5, 127.3, 126.9, 123.9, 120.8, 119.4, 118.3, 117.9, 115.5, 115.3, 111.4, 108.9, 56.6, 28.3. ^{19}F NMR (376 MHz, DMSO- d_6) δ , ppm: –111.9 (m). HRMS (TOF MS ES+): calcd for $\text{C}_{24}\text{H}_{21}\text{FN}_3\text{O}_3\text{S}$ ($[\text{M} + \text{H}]^+$), 482.1186; found 482.1183.

Synthesis of Labeling Precursors. The reaction of oxidative formation of iodonium compound was adapted from the published procedure.¹⁵

(4-Carboxyphenyl)(4-methoxyphenyl)iodonium 4-methylbenzenesulfonate (21). 4-Iodobenzoic acid methyl ester (10 g, 38.2 mmol), 3-chloroperoxybenzoic acid (17.8 g, 72 mmol), and anisole (6.2 g, 57.2 mmol) were dissolved in dichloromethane/trifluoroethanol (1:1, 200 mL). 4-Toluenesulfonic acid (10.89 g, 57.2 mmol) was added, and the reaction mixture was stirred at room temperature for 3 days. To the obtained suspension ether (1500 mL) was added and the precipitate was filtered and washed with ether. The solvent was evaporated to yield 22.8 g of the crude intermediate methyl ester. MS (ES+): m/z 368.61 ($[\text{M}]^+$) (iodonium cation).

The methyl ester was dissolved in TFA/water (1:1, 600 mL) and heated at 120 °C (oil bath) for 48 h. After cooling to room temperature, the solvents were removed and the oily residue was triturated with ether (500 mL), filtered, and dried to give an off-white solid (18.5 g, 35.1 mmol, 92%). ^1H NMR (400 MHz, DMSO- d_6) δ , ppm: 13.50 (br. s., 1 H), 8.34–8.25 (m, 2 H), 8.24–8.15 (m, 2 H), 8.04–7.94 (m, 2 H), 7.47 (d, J = 8.1 Hz, 2 H), 7.15–7.02 (m, 4 H), 3.80 (s, 3 H), 2.28 (s, 3 H). ^{13}C NMR (101 MHz, DMSO- d_6) δ , ppm: 166.1, 162.1, 145.8, 137.5, 137.4, 134.9, 133.6, 131.9, 128.0, 125.5, 121.3, 117.5, 105.4, 55.7, 20.8. MS (ES+): m/z 355.11 ($[\text{M}]^+$) (iodonium cation). MS (ES–): m/z 171.07 ($[\text{M}]^-$) (tosylate anion).

Methyl N-([4-((4-(4-Methoxyphenyl)iodonio)benzoyl)amino)phenyl]sulfonyl)-D-tryptophanate Salts (23b–e). Aniline I (200 mg, 0.54 mmol), (4-carboxyphenyl)(4-methoxyphenyl)iodonium 4-methylbenzenesulfonate 21 (423 mg, 0.8 mmol), and 1-(3-dimethylaminopropyl)-3-ethylcarbodiimide hydrochloride (1.03 g, 5.4 mmol) were suspended in acetonitrile/pyridine (2:1, 30 mL), and the reaction was stirred at room temperature for 4 days. The resulted clear yellow solution was acidified to pH 1 using 2N aqueous HCl. The solution was extracted with dichloromethane (3 \times 200 mL), and the organic phases were combined, dried (MgSO_4), and concentrated. The residue was dissolved in water/acetonitrile (1:1, 10 mL). Toluenesulfonic acid monohydrate (101 mg, 0.53 mmol) was added, and the mixture was lyophilized (^1H NMR indicated an excess of tosylate in this material). The product (12 mg) was stirred in dichloromethane, filtered, and dried to obtain the title compound as approximately 35–40% tosylate salt based on ^1H NMR. The remaining 60–65% were assumed to be the corresponding chloride salt. The yield, when calculated for both counterions together, was in a range of 70–80%. ^1H NMR (400 MHz, DMSO- d_6) δ , ppm: 10.94–10.81 (m, 1 H), 10.70 (s, 1 H), 8.41 (d, J = 8.6 Hz, 1 H), 8.30 (d, J = 8.3 Hz, 2 H), 8.19–8.09 (m, 2 H), 8.00–7.91 (m, J = 8.6 Hz, 2 H), 7.87–7.79 (m, J = 8.8 Hz, 2 H), 7.65–7.57 (m, J = 8.8 Hz, 2 H), 7.48 (d, J = 8.1 Hz, 0.8 H, tosylate), 7.26 (d, J = 7.8 Hz, 1 H), 7.29 (d, J = 8.1 Hz, 1 H), 7.13–6.99 (m, 5 H), 6.96–6.89 (m, 1 H), 3.96 (q, J = 7.6 Hz, 1 H), 3.78 (s, 3 H), 3.33 (s, 3 H), 3.04 (dd, J = 7.5, 14.3 Hz, 1 H), 2.88 (dd, J = 7.1, 14.4 Hz, 1 H), 2.28 (s, 1.1 H, tosylate). ^{13}C NMR (101 MHz, DMSO- d_6) δ , ppm: 171.4, 164.9, 161.6, 145.7, 142.2, 137.6, 137.0, 137.0, 136.0, 135.1, 134.6, 130.3, 128.0, 127.3, 126.7, 125.5, 123.9, 123.1, 120.9, 119.6, 118.4, 117.6, 117.2, 111.5, 108.6, 108.3, 56.7, 55.6, 51.7, 28.2, 20.8. MS (ES+): m/z 710.22 ($[\text{M}]^+$) (iodonium cation). MS (ES–): m/z 171.03 ($[\text{M}]^-$) (tosylate anion).

Introduction of Counterions. The synthesis was conducted as described above (scale: 2 g of aniline I). After completion of the

reaction and without any workup, the reaction mixture was concentrated and the residue was adsorbed on LiChroprep RP18 packing material (Merck), charged on a RP-18 PuriFlash 15PT C18T column (Interchim) and eluted consecutively with the following solvents:

- (1) an aqueous 0.1% solution H-X (X = tosylate, bromide, triflate, or perchlorate, according to the desired salt form) (500 mL/1 g crude product);
- (2) water (500 mL/1 g crude product);
- (3) a gradient of acetonitrile in water, from 20% to 90% over 20 min.

The product was collected by monitoring UV signal (215–360 nm, PDA detector) and lyophilized.

Tosylate (23b). The analytical data correspond to those described above; integrals of the tosylate signals indicate the presence of 0.9–1.0 equiv tosylate with respect to the cation.

Triflate (23c). The triflate could be qualitatively confirmed by ^{19}F NMR δ –77.7 and ^{13}C NMR δ 120.7 (q, J = 322 Hz). Because tosylate could not be detected, a complete exchange to triflate was presumed.

Bromide (23d). The presence of bromide was not directly confirmed. Because the tosylate, which was present in the crude product, could not be detected, a complete exchange to bromide was presumed.

Perchlorate (23e). The presence of perchlorate was not directly confirmed. Because the tosylate, which was present in the crude product, could not be detected, a complete exchange to perchlorate was presumed.

Enantiomeric Stability under Basic Hydrolysis Conditions. Methyl ester of compound 7 was hydrolyzed under conditions similar to the hydrolysis reaction during radiosynthesis. For this, 20 mg of the methyl ester, 26 mg of Cs_2CO_3 , 5 mL pf DMF, and 100 μL of water were combined in a reaction vial. Then, 1 mL of 4N NaOH was added and the mixture was heated on an oil bath at 100 °C for 10 or 20 min. The reactions were removed from the oil bath and neutralized with 4 mL of 1N HCl to pH = 7.5. Analysis on chiral HPLC confirmed that the reactions were chemically clean and full conversion occurred at both time points. The product eluted at 4.0 min, which corresponds to R-enantiomer. The expected retention time for the S-enantiomer was 6.25 min.

Inhibitory Potency Determination (Fluorescent Assay). Recombinant human full length MMP2 (902-MP, R&D Systems) or MMP9 (911-MP, R&D Systems) was chemically activated using *p*-aminophenylmercuric acetate (APMA) according to the manufacturer's protocol.²¹ To the activated enzyme (final concentration 0.1 nM, 24 μL) in reaction buffer (50 mM Tris/HCl pH 7.5, 10 mM CaCl_2 , 150 mM NaCl, 0.05% Brij-35), compound of interest (in DMSO, suitable concentrations, e.g., 1 nM to 30 μM , 1 μL) was added in a 384-MTP white plate. Reaction was started by addition of internally quenched substrate Mca-Pro-Leu-Gly-Leu-Dpa(Dnp)-Ala-Arg-NH₂ (final concentration 10 μM ; Mca = (7-methoxycoumarin-4-yl)acetyl; Dpa(Dnp) = N-3(2,4-dinitrophenyl)-L-2,3-diaminopropionyl, R&D Systems) to yield a total volume of 50 μL . Progress of the MMP reaction was monitored by fluorescence intensity measurement (excitation, 320 nm; emission, 410 nm) over 120 min at 32 °C. IC₅₀ values were determined by plotting the compound concentration versus the percentage of MMP activity by interpolation.

^{18}F -Fluoride Production. No-carrier-added (nca) ^{18}F -fluoride was produced via the $^{18}\text{O}(\text{p,n})^{18}\text{F}$ nuclear reaction in a fixed-energy Cyclone 18/9 cyclotron (IBA, Belgium). For this, >98% isotopically enriched ^{18}O -water (Nukem GmbH, Germany) was irradiated by 18 MeV proton beam. Produced ^{18}F -fluoride/ ^{18}O -water solution was transferred using a helium stream from the target to a shielded hot cell equipped with a manipulator where radiosynthesis was performed. Typical production of ^{18}F -fluoride at end of bombardment (EOB) of the 2.5 mL target for 20 mAh (~45 min) was 47–60 GBq.

Radiochemistry. ^{18}F -fluoride (~ 80–100 GBq) was trapped on an anion exchange Sep-Pak Light Accell Plus QMA cartridge (Waters) preconditioned with 5 mL of 0.5 M potassium carbonate solution, 10 mL of water, and flushed with 10 mL of air. It was eluted with 1 mL

solution of cesium carbonate (2.6 mg) in acetonitrile/water (1:1). Effluent was collected to a tightly closed 5 mL Reacti-Vial (Thermo Fisher Scientific), and solvent was evaporated under a stream of nitrogen and reduced pressure (50–80 mbar) at 100 °C for 10 min. The residue was azeotropically dried by addition of 3 × 0.8 mL anhydrous acetonitrile. Precursor (**22a–b**, **23b–e**) (~2 mg, 2.5 ± 0.2 μmol) predissolved in 500 μL of DMSO, containing 10 μL of water, was added to the dry ¹⁸F-fluoride, and the reaction mixture was heated at 100 °C for 3 min. After cooling for 5 min at room temperature, the reaction mixture was diluted with 1 mL of water and loaded into semipreparative HPLC. The radioactive fraction containing the product was collected into 30 mL of water and passed through a Sep-Pak Light C18 cartridge (preconditioned in advance with 5 mL of ethanol followed by 10 mL of water). The cartridge was washed with additional 5 mL of water for injection to remove traces of ¹⁸F-fluoride. The product was eluted with 0.5 mL of ethanol to a penicillin vial. The ethanol fraction was diluted with 9.5 mL of PBS and passed through a 13 mm Nalgene 0.2 μm sterile filter (Thermo Fisher Scientific) to a sterile vial, giving an injectable sterile solution containing 5% ethanol by volume, which was used for biological experiments. An aliquot of known volume and radioactivity of the final formulated solution was injected into analytical HPLC for quality control, which required approximately 20 min. The retention time of the radiolabeled product, ¹⁸F-7, was in a range 10.67–10.72 min. The specific radioactivity was determined from the quality control run matching the area of the UV absorbance peak at 254 nm, which coeluted with the radiolabeled product, to a standard calibration curve calculated using known concentrations of the nonradioactive reference compound 7.

Evaluation of the Stability in Human and Rodent Plasma in Vitro. An aliquot of 50 μL (~60 MBq) of ¹⁸F-7 formulated solution was added to human or rodent plasma (~0.5 mL) and vortexed. The mixture was distributed into six Eppendorf microcentrifuge tubes, 70 μL (~7 MBq) to each. The first tube, which represented zero time point, contained 70 μL of methanol. Five other tubes were incubated at 37 °C in an Eppendorf Thermomixer Compact (Vaudaux-Eppendorf) shaker. The samples were quenched with 70 μL of ice-cold methanol, one by one, at 5, 30, 60, 90, and 120 min. Plasma proteins were precipitated by centrifugation at 10000g for 10 min. The supernatants were analyzed using UPLC.

Animal Care. Animal care and all experimental procedures were approved by the Veterinary Office of the Canton Zurich. Female C57BL/6 mice (6 weeks old, Charles River) were allowed free access to food and water.

Evaluation of the Metabolic Stability in Vivo. C57BL/6 mice were injected with 150 μL of 650 MBq/mL (17.5 mCi/mL) ¹⁸F-7 solution each. The mice were sacrificed by decapitation at 15, 30, and 60 min after injection and blood and urine were collected. The proteins were precipitated with twice the volume of ice-cold acetonitrile. After centrifugation, the supernatants were injected into UPLC for analysis.

In Vivo PET/CT Imaging. A C57BL/6 mouse was injected with 5.3 MBq ¹⁸F-7 into a tail vein and anesthetized with 2–3% isoflurane in oxygen/air. Body temperature was maintained at 37 °C with warm air. The mouse was scanned in a GE/Sedecal eXplore VISTA PET/CT (4.8 cm axial field of view) in two-bed static PET acquisition mode with the anterior part from 8–22 min and the posterior part 23–38 min after injection. A CT was added for anatomical orientation. Raw data were reconstructed with a voxel size of 0.3875 × 0.3875 × 0.775 mm³. Images were generated with PMOD software (PMOD Technologies).

■ ASSOCIATED CONTENT

■ Supporting Information

Synthetic procedures and spectroscopic characterization of aniline **I**, aniline **II**, and compounds **6**, **8–20**, **22a**, and **22b**. ¹H, ¹³C, and ¹⁹F NMR spectra of MMP inhibitor **7** and its labeling precursor **23d**. UPLC chromatograms of mouse blood and urine 60 min after injection of ¹⁸F-7. This material is available free of charge via the Internet at <http://pubs.acs.org>.

■ AUTHOR INFORMATION

Corresponding Author

*For S.M.A.: phone, +41 44 633 7463; E-mail, simon.ametamey@pharma.ethz.ch. For S.V.S.: phone, +41 44 633 7492; E-mail, svetlana.selivanova@pharma.ethz.ch, selivanova@usherbrooke.ca.

Present Address

[§]L.M.D.: Piramal Imaging, Berlin, Germany.

Author Contributions

^{||}These authors contributed equally.

Notes

The authors declare no competing financial interest.

■ ABBREVIATIONS USED

MMP, matrix metalloproteinase; TIMP, tissue inhibitor of metalloproteinase; PET, positron emission tomography; CT, computed tomography; EOB, end of bombardment; EOS, end of synthesis; RCY, radiochemical yield; SUV, standardized uptake value; APMA, 4-aminophenylmercuric acetate; TFA, trifluoroacetic acid; DMF, dimethylformamide; DMSO, dimethylsulfoxide; HPLC, high performance liquid chromatography; UPLC, ultra performance liquid chromatography; NMR, nuclear magnetic resonance; HRMS, high resolution mass spectrometry

■ REFERENCES

- (1) Newby, A. C. Metalloproteinases and vulnerable atherosclerotic plaques. *Trends Cardiovasc. Med.* **2007**, *17*, 253–258.
- (2) Deguchi, J.; Aikawa, M.; Tung, C.-H.; Aikawa, E.; Kim, D.-E.; Ntziachristos, V.; Weissleder, R.; Libby, P. Inflammation in atherosclerosis: visualizing matrix metalloproteinase action in macrophages in vivo. *Circulation* **2006**, *114*, 55–62.
- (3) Ibarra, J. M.; Jimenez, F.; Martinez, H. G.; Clark, K.; Ahuja, S. S. MMP-activated fluorescence imaging detects early joint inflammation in collagen-antibody-induced arthritis in CC-chemokine receptor-2-null mice, in vivo. *Int. J. Inflammation* **2011**, *2011*, article ID 691587, doi:10.4061/2011/691587.
- (4) Wagner, S.; Breyholz, H.-J.; Faust, A.; Höltke, C.; Levkau, B.; Schober, O.; Schäfers, M.; Kopka, K. Molecular Imaging of matrix metalloproteinases in vivo using small molecule inhibitors for SPECT and PET. *Curr. Med. Chem.* **2006**, *13*, 2819–2838.
- (5) Furumoto, S.; Takashima, K.; Kubota, K.; Ido, T.; Iwata, R.; Fukuda, H. Tumor Detection Using F-18-labeled matrix metalloproteinase-2 inhibitor. *Nucl. Med. Biol.* **2003**, *30*, 119–125.
- (6) Fei, X.; Zheng, Q.-H.; Liu, X.; Wang, J.-Q.; Sun, H. B.; Mock, B. H.; Stone, K. L.; Miller, K. D.; Sledge, G. W.; Hutchins, G. D. Synthesis of radiolabeled biphenylsulfonamide matrix metalloproteinase inhibitors as new potential PET cancer imaging agents. *Bioorg. Med. Chem. Lett.* **2003**, *13*, 2217–2222.
- (7) Kuhnast, B.; Bodenstein, C.; Wester, H. J.; Weber, W. Carbon-11 labelling of an N-sulfonylamino acid derivative: a potential tracer for MMP-2 and MMP-9 imaging. *J. Label. Compd. Radiopharm.* **2003**, *46*, 539–553.
- (8) Zheng, Q.-H.; Fei, X.; Liu, X.; Wang, J.-Q.; Stone, K. L.; Martinez, T. D.; Gay, D. J.; Baity, W. L.; Miller, K. D.; Sledge, G. W.; Hutchins, G. D. Comparative studies of potential cancer biomarkers carbon-11 labeled MMP inhibitors (S)-2-(4'-[¹¹C]methoxybiphenyl-4-sulfonylamino)-3-methylbutyric acid and N-hydroxy-(R)-2-[(4'-[¹¹C]methoxyphenyl)sulfonyl]benzylamino]-3-methylbutanamide. *Nucl. Med. Biol.* **2004**, *31*, 77–85.
- (9) Breyholz, H.-J.; Wagner, S.; Faust, A.; Reimann, B.; Höltke, C.; Hermann, S.; Schober, O.; Schäfers, M.; Kopka, K. Radiofluorinated pyrimidine-2,4,6-triones as molecular probes for noninvasive MMP-targeted imaging. *ChemMedChem* **2010**, *5*, 777–789.

(10) Schrigten, D.; Breyholz, H.-J.; Wagner, S.; Hermann, S.; Schober, O.; Schafers, M.; Haufe, G.; Kopka, K. A new generation of radiofluorinated pyrimidine-2,4,6-triones as MMP-targeted radiotracers for positron emission tomography. *J. Med. Chem.* **2012**, *55*, 223–232.

(11) Tamura, Y.; Watanabe, F.; Nakatani, T.; Yasui, K.; Fuji, M.; Komurasaki, T.; Tsuzuki, H.; Maekawa, R.; Yoshioka, T.; Kawada, K.; Sugita, K.; Ohtani, M. Highly selective and orally active inhibitors of type IV collagenase (MMP-9 and MMP-2): *N*-sulfonylamino acid derivatives. *J. Med. Chem.* **1998**, *41*, 640–649.

(12) Bégue, J.-P.; Bonnet-Delpon, D. *Bioorganic and Medicinal Chemistry of Fluorine*; John Wiley & Sons: New York, 2008; p 15.

(13) Cai, L.; Lu, S.; Pike, V. W. Chemistry with [¹⁸F]fluoride ion. *Eur. J. Org. Chem.* **2008**, 2853–2873.

(14) Okuyama, T.; Takino, T.; Sueda, T.; Ochiai, M. Solvolysis of cyclohexenyliodonium salt, a new precursor for vinyl cation: remarkable nucleofugality of the phenyliodonio group and evidence for internal return from an intimate ion–molecule pair. *J. Am. Chem. Soc.* **1995**, *117*, 3360–3367.

(15) Zhu, M.; Jalalian, N.; Olofsson, B. One-pot synthesis of diaryliodonium salts using toluenesulfonic acid: a fast entry to electron-rich diaryliodonium tosylates and triflates. *SynLett* **2008**, 592–596.

(16) Wadsworth, H. J.; Devenish, T. Fluoridation method. WO 2005/097713, 2005.

(17) Chun, J.-H.; Lu, S.; Lee, Y.-S.; Pike, V. W. Fast and high-yield microreactor syntheses of *ortho*-substituted [¹⁸F]fluoroarenes from reactions of [¹⁸F]fluoride ion with diaryliodonium salts. *J. Org. Chem.* **2010**, *75*, 3332–3338.

(18) Wadsworth, H. J.; Widdowson, D. A.; Wilson, E.; Carroll, M. A. Radical trap in fluoridation of iodonium salt. WO 2005/061415, 2005.

(19) Carroll, M. A.; Nairne, J.; Smith, G.; Widdowson, D. A. Radical scavengers: a practical solution to the reproducibility issue in the fluoridation of diaryliodonium salts. *J. Fluorine Chem.* **2007**, *128*, 127–132.

(20) Ross, T. L.; Ermert, J.; Hocke, C.; Coenen, H. H. Nucleophilic ¹⁸F-fluorination of heteroaromatic iodonium salts with no-carrier-added [¹⁸F]fluoride. *J. Am. Chem. Soc.* **2007**, *129*, 8018–8025.

(21) Merck Millipore: *Organomercurial Activation Protocol*; Merck, <http://www.millipore.com/catalogue/item/PF038-10UG=BIOS-S-EPDF-1033-1111-RC>.